Desalination and Water Treatment
www.deswater.com
doi: 10.5004/dwt.2022.28013

246 (2022) 291–303
January

Removal of Basic Blue 41 by waste product from the phosphate industry: batch design and regeneration

Mariem Bembli[a,b], Fethi Kooli[c,*], Ramzi Khiari[d], Khaled Boughzala[a,b,*]

[a]*Unité de recherche- Analyses et Procédés Appliqués à l'environnement, Institut Supérieur des Sciences Appliquées et Technologie de Mahdia, 5121 Mahdia, Tunisia, email: khaledboughzala@gmail.com*
[b]*Unit Electrochemistry, Materials and Environment, University of Kairouan, 3100, Kairouan, Tunisia*
[c]*Department of Chemistry, Faculty of Science, Islamic University of Madinah, Al-Madinah Al-Munawwarah 42351, Saudi Arabia, email: fethi_kooli@yahoo.com*
[d]*University of Monastir, Laboratory of Environmental Chemistry and Cleaner Process (LCE2P- LR21ES04), 5019 Monastir, Tunisia,*

Received 21 July 2021; Accepted 22 November 2021

ABSTRACT

To reduce the environmental impact of phosphate waste product, these materials were proposed as a removal agent of a colored Basic Blue 41 dye (BB-41) from artificially contaminated solution. The effect of calcination of this waste was also investigated on its removal properties. These materials were characterized beforehand, as is intended for the removal tests, by chemical analysis, powder X-ray diffraction, Fourier-transform infrared spectroscopy, thermogravimetric analysis–differential thermal analysis, scanning electronic microscopy, and N_2 adsorption isotherms. The phosphate waste rock exhibited higher removal capacity of 207 mg g^{-1} of BB-41 than the natural rock with a value of 57 mg g^{-1} of BB-41, as estimated from Langmuir model. Upon calcination, the removal capacities were reduced by 22%–60%, depending of heating temperatures. Higher removal amounts were achieved at pH values greater than 7. The removal procedure was found to be spontaneous and endothermic process. 60%–80% removal efficiency was maintained after four cycles of regeneration, depending on the spent byproducts. A single stage batch absorber was designed based on the optimum Freundlich isotherm. For example, the masses of 237 and 542 g for phosphate waste and natural phosphate rocks were required to reduce the BB-41 amount of 90% in 10 L of solution with an initial concentration of 200 mg L^{-1}.

Keywords: Natural phosphate rocks; Removal; Basic Blue 41; Regeneration; Batch design

1. Introduction

Synthetic dyes have been used in several industrial sectors such as the automotive sector, the textile industries, leather tanning, plastics, paper, and photoelectrochemical cells and therefore, a huge amount of water is consumed [1]. Discarded colored wastewater poses an ecological problem if it is discharged directly into natural stream of water. These dyes damage the quality of water bodies, the aquatic ecosystem, and the biodiversity in the environment [2,3]. Their elimination is imperative [4]. Several techniques for the treatment and depollution of textile effluents were reported in the literature. It is important to mention, among them, the membrane filtration techniques [5], coagulation/flocculation [6], electro-coagulation [7], oxidation techniques

* Corresponding authors.

[8], aerobic biological processes, and anaerobes [9,10]. These established processes have inherent limitations such as design complexity and financial inputs, thus it is necessary to look for efficient and simple methods. An abundance of studies has been conducted and supported that adsorption belongs to the more effective method for dye removal from aqueous effluents, due to its positive points such availability of raw cheap absorbents, simple operation, the design, and insensitive of toxic substances [11].

Numerous studies have reported the retention of colorant Basic Blue 41 using sulfonic acid based polymeric membrane [12], agro-industrial wastes [13], rice stems [14], raw and modified clay minerals, waste bricks [15,16], and different biosorbents [17–19].

The natural phosphate (NP) is an abundant product extracted from phosphate rocks and makes up of carbonated fluoroapatite with important substitution of phosphate by carbonate [20]. It is used in the production of phosphoric acid, after a washing process and reaction with sulfuric acid [21]. This process is called a wet process, because concentrated solution of sulfuric acid (93%) was used to digest the apatite ore [22]. Another important use of the phosphate rocks is the production of fertilizers [23]. The element phosphorus is important because it is an essential component of energy metabolism of all forms of life, with nitrogen, potassium, and phosphorus present the three macronutrients needed by all crops.

The production of phosphoric acid and phosphate fertilizers from phosphate rocks resulted in the formation of huge amount of wastes by products such as phospohogypsum [24.]. Some evaluation of theses wastes was proposed in the treatment of polluted water and some research activities have studied their utility as removal agents of some dyes and heavy metal ions from aqueous solutions [25–34]. In addition, significant amounts of phosphate discharges called poor are unusable, represent a serious problem for the phosphate industry.

The calcination (heat treatment) of natural phosphate rocks was described in the literature for upgrading the calcareous phosphate ores [35], and to propose other applications than direct synthesis of fertilizers, such the production of pure chemicals, soft drinks and pharmaceutical products [36]. The use the calcined materials were documented in the synthesis of fertilizers. However, there are no reports, related to their use in the elimination of dyes from artificially contaminated water.

In this study, the waste by product (PWR) with or without calcination was investigated as removal agent for the Basic Blue 41 (BB-41), the dye was selected as a model dye due to its diverse applications in different fields, such as the textile and leather industries. In addition, it exhibits concerns related to the health of living things and aquatic environment [37]. The first step consists to characterize the removal solids by several techniques such, elemental analysis, X-ray diffraction, Fourier-transform infrared spectroscopy (FTIR), thermogravimetric analysis, and surface area properties. The second step is to investigate their removal properties for Basic Blue 41 dye. Different parameters were varied to study their effect on the removal properties, among them the pH of the dye solution, its initial concentration, temperature of adsorption, and the dosage of the used solids. Different models were used to fit the experimental data. Computational calculations were performed to propose a possible removal mechanism. Furthermore, the regeneration efficiency of the spent materials was investigated by using high-efficiency and low-cost process [15]. The close the gap between the small scale laboratory data and the application in real cases, design batch adsorber was proposed based on the Freundlich model.

2. Materials and methods

2.1. Materials

Natural phosphate was taken from the Gafsa–Metlaoui Basin (denoted as the NP sample). phosphate waste rock (denoted as PWR) is a byproduct of a phosphate company's washing plant. Prior to use, the samples have been considerably washed with distilled water, then dried in an oven at 105°C.

The natural phosphate (NP) and phosphate waste rock (PWR) were exposed to thermal activation under nitrogen (150 mL h^{-1}) at two different temperatures (400°C or 1,000°C) at 5°C/min for 2 h. The products obtained were assigned NP400, NP1000, PWR400 and PWR1000, respectively. All the compounds were intended for the removal tests of the Basic Blue 41 dye.

The Basic Blue 41 dye (BB-41) used for the study was bought from a local dye dealer. It has the molecular formula $C_{20}H_{26}N_4O_6S_2$ (mol. weight. 482.57 g mol^{-1}). The supernatant of the sample is determined by UV–visible spectroscopy (Perkin Elmer model LAMBDA20) at its maximum absorbance wavelength of 606 nm.

The cobalt nitrate hexa-hydrate ($Co(NO_3)_2{\cdot}6H_2O$) and Oxone ($2KHSO_5{\cdot}KHSO_4{\cdot}K_2SO_4$, 4.7% active oxygen) were used without further treatment after purchase from Alfa Aesar. In all the experiments, the bi-distilled water was used.

2.2. Removal experiments

The removal of the BB-41 dye was performed by a batch equilibrium method to evaluate the optimum operational conditions for the BB-41, and they are summarized in Table 1. Different concentrations (varying from 5 to 400 mg L^{-1}) were achieved by the dilution of stock solution (with a concentration of 1,000 mg L^{-1}). Then, 0.1 g of the solid was added to a total volume of 200 mL (dye solution) under a shacking speed of 150 rpm, without changing the pH of the starting solution (6.50, used as natural pH) for overnight.

The removed quantity (q_e, mg g^{-1}) and the removal percentage were determined by Eqs. (1) and (2), respectively.

$$q_e = \left(C_i - C_e\right)\frac{V}{m} \tag{1}$$

$$R\% = \frac{\left(C_i - C_e\right)}{C_i} \times 100 \tag{2}$$

where C_i and C_e correspond to the initial and the equilibrium concentrations of BB-41 dye (mg L^{-1}), respectively.

Table 1
Experimental studies for the removal of Basic Blue 41

No.	Study	Parameters
1	Effect of initial BB-41 concentration	BB-41 initial concentration in the range of 5 to 400 mg L^{-1}. Mass of solid 0.1 g. Used volume of 200 mL, natural pH.
2	Effect of calcination temperature of waste	Waste solids were calcined at 400°C and 1,000°C same procedure than study No 1.
3	Effect of solid dosage	PWR was varied from 0.05 to 1.5 g in 200 mL of C_i = 100 mg L^{-1}.
4	Effect of BB-41 pH solution	pH was varied between 2.5 to 11, dose of solid 0.1 g added to 200 mL aqueous solution with C_i of 100 mg L^{-1}.
5	Equilibrium studies	Evaluation of maximum removal amounts and fitting the experimental data by isotherm models.
6	Effect of temperature on the removal of BB-41	BB-41 C_i of 120 mg L^{-1} with 50 mg and contact time of 2 h at 30°C, 45°C, 60°C, and 75°C.
7	Regeneration studies	Tests were studied using 0.4 g of NP or PWR treated in 200 mL of C_i = 200 mg L^{-1}.

V is the used solution volume (L) and m is the material mass (mg). For evaluating the effect of different parameters on the removal of BB-41, the dosage of adsorbents, initial dye concentrations, contact time, temperature, and pH were varied independently.

The isotherm models used to determine the best-fitted model was nonlinear regression. Two error functions were assessed: nonlinear chi-square test χ^2 and coefficient of determination (R^2) (3). The nonlinear function was fitted by the method of nonlinear-least squares.

$$\chi^2 = \sum \left(\frac{q_{cal} - q_{exp}}{q_{exp}} \right)^2 \quad (3)$$

2.3. Theoretical calculation (modelling approach)

The computations were made with a P4 Duo Processor X64 (8G RAM) microcomputer in Windows 8.0 environment. All calculations were made using HyperChem v7 software (http://www.hyperchem.com). The geometry of Basic Blue 41 was optimized at the MM+ level of theory (r.m.s = 0.00941 kcal/mol/Å). Mulliken atomic charges and electrostatic potential were assessed by the semi-empirical parametric method 3 (PM3) being derived from the Hartree-Fock theory [27].

2.4. Regeneration of spent byproducts

Pristine NP or PWR samples (0.4 g) were added to 200 mL of a fresh solution of BB-41 (C_i = 200 mg L^{-1}) and left overnight. The used solid was separated by centrifugation and treated with a 10 mL solution of $Co(NO_3)_2 \cdot 6H_2O$ and 12 mg of oxone ($2KHSO_5 \cdot KHSO_4 \cdot K_2SO_4$). The cobalt cations ($Co^{2+}$) behaved as a homogeneous catalyst. The oxidant (oxone) was added to the mixture and it allows to degrade the fixed BB-41 dyes on the surface. The treated solid was centrifuged, rinsed few times with deionized water, then reused in the next cycle. The mixture of cobalt and Oxone solution was not discharged and utilized in the next recycle runs [15].

2.5. Characterization

The chemical composition of the investigated materials was analyzed using atomic absorption spectroscopy (Perkin-Elmer 3110). Powder X-ray diffraction (XRD) analysis of the materials was conducted using an X'Pert Pro, PANalytical diffractometer operating with Cu Kα radiation. The samples were scanned from a starting angle (2θ) of 5° to an end angle (2θ) of 80°. The identification of the mineral phases was carried out using the data given in the ASTM cards. FTIR spectra were achieved using a Perkin-Elmer 1283 spectrometer with the KBr pellet technique. Thermal gravimetric analysis was performed using a Seteram Instrumentation SETSYS evolution system with a heating rate of 10°C/min up to 1,000°C under an atmosphere air. Surface morphology of the samples was analyzed by scanning electronic microscopy (SEM, FEI Quanta 200). The specific surface area values were estimated from nitrogen adsorption isotherms using the BET (Brunauer–Emmett–Teller) equation. The isotherms were obtained using a Micromeritics ASAP 2020 system. The samples were degassed at 120°C for 8 h prior to the measurement. The pH_{zpc} of the NP, and PWR samples was measured in solutions of NaCl (0.01 mol L^{-1}). The concentration of BB-41 at equilibrium was determined during the removal runs using a UV-visible spectrophotometer (Perkin Elmer model LAMBDA20) at a maximum wavelength of 606 nm.

3. Results and discussion

3.1. Characterization of used solids

The results of the chemical analysis are given in Table 2. It is noted that the maximum CaO concentration (45%) is present in NP and it decreases to 26.7% in the PWR sample. The NP sample has a high P_2O_5 content (25.6%) compared to PWR sample (14.0%). The content of P_2O_5 in NP was close to that reported for similar rocks [27,28]. The decrease of CaO and P_2O_5 contents was related to washing process. A small percentage of MgO, from 0.87% to 2.15%, was detected. The Ca/P atomic ratio is about 1.75 for NP sample, and

about 1.91 for PWR [38]. This variation was due to lower amount of P_2O5 in PWR, resulted from the washing process. The Cd content varied between 45 and 51 ppm. The thermal treatment (calcination) did not change dramatically the chemical composition, and slight variation in P_2O_5 was observed for other phosphate rocks [39].

Fig. 1 depicts the powder XRD patterns of the raw NP and PWR samples. The NP and PWR specters exhibited similar patterns. Mineralogical identification reveals that both powders contained mainly as a major phase of carbonate fluoroapatite, with traces of francolite $Ca_{9.55}(PO_4)_{4.96}F_{1.96}(CO_3)_{1.28}$, heulandite $((C_2H_5)NH_3)_{7.85}(Al_{8.7}Si_{27.3})O_{72})(H_2O)_{6.92})$ and Quartz (SiO_2) [28]. After calcination, at 400 and 1,000°C, no variation of the major phase was observed, and mainly carbonate fluoroapatite was detected. The good resolution of the reflections indicated a certain level of crystallinity of the calcined materials [40].

The FTIR spectra of the samples are shown in Fig. 2. The spectra of NP and PWR samples exhibited characteristic bands due to the PO_4^{3-} and CO_3^{2-} ions. The bands observed around 1,042 and 890 cm^{-1} assigned to the stretching vibration modes P–O, while the bands between 570 and 470 cm^{-1} are consistent with the bending mode O–P–O. Those appearing in the range between 1,500 and 1,400 and at 863 cm^{-1} [41] are assigned to vibration modes of the CO_3^{2-} groups. These bands indicate that the CO_3^{2-} ions were not incorporated into the structure of the material. The bands of quartz phase (1,042 and 474 cm^{-1}) could be overlapped with those of PO_4 groups [28]. Additional bands in the range from 3,700 to 3,000 cm^{-1} and at 1,640 cm^{-1}, were associated to water molecules adsorbed on the particle's surface [28].

FTIR spectra indicated some chemical changes occurred for the calcined materials at 1,000°C, They exhibited an intense peak around at 1,036 cm^{-1} with a shoulder at 1,081 cm^{-1} corresponding to the phosphorous group (PO_4^{3-}). The bands related to carbonate species and impurities vanished at 1,440 cm^{-1}. Shoulder band arround 3,440 cm^{-1} was related to physiadsorbed water on the surfaces of the calcined materials.

The thermal features of the NP and PWR samples are given in Fig. 3. The TG features of the NP and PWR samples display three successive mass losses. The first thermal event occurs between room temperature and 150°C and is caused by water desorption. It is associated with an endothermic effect that is observed on the differential thermal analysis (DTA) curve at 85°C and 100°C, with a shoulder at 140°C. The second mass loss corresponds to the loss of water content and dehydroxylation from 170°C to 450°C, with a broad endothermic effect that is evidenced on the DTA curve at around 350°C [28,42]. The third weight loss event, which starts at 400°C and continues to 1,000°C, is attributed to the decomposition of carbonates and other materials [42]. Two broad exothermal peaks are detected in the range of 700°C–750°C and are associated with the phase transformation of some resulting products. The PXRD and FTIR data confirmed these mass losses.

The NP and PWR materials exhibited specific surface areas of 11.35 and 26.02 $m^2\ g^{-1}$, respectively. These values are close to those reported for natural phosphate rocks [43]. The slight difference between the S_{BET} value of the PWR material could be related to the washing

Table 2
Chemical analysis of the main elements in used samples

Samples	NP	PWR
P_2O_5 (%)	25.64	14.01
CaO (%)	44.94	26.72
MgO (%)	0.87	2.15
Cd (ppm)	45	51
CaO/P_2O_5	1.75	1.90

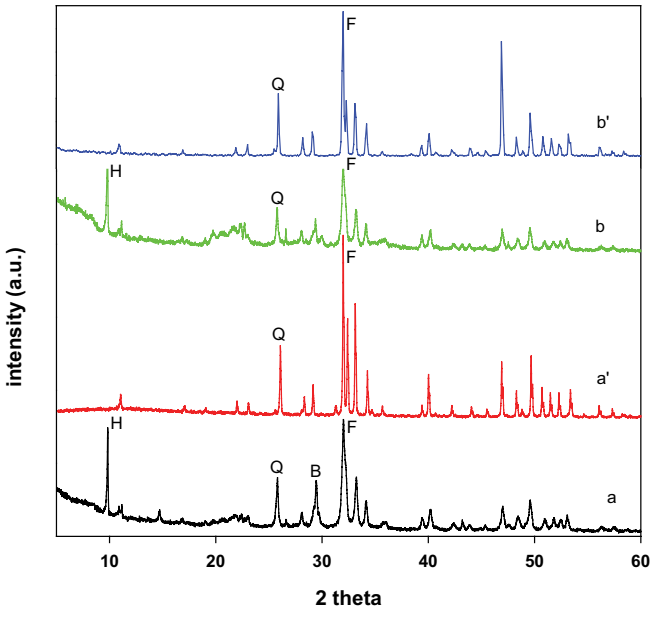

Fig. 1. Powder XRD patterns of (a) natural phosphate and (b) phosphate waste rock. Corresponds (H) to heulandite, (F) to carbonate fluoroapatite, and (Q) to quartz phases. (a′ and b′) correspond to sample (a and b) calcined at 1,000°C.

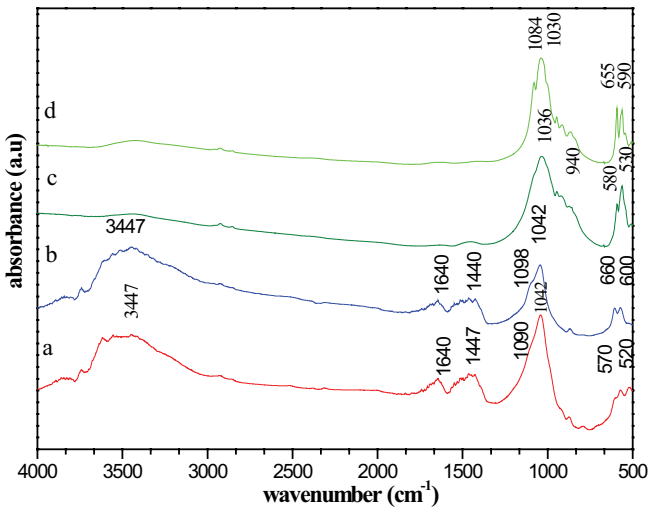

Fig. 2. FTIR spectra of (a) natural phosphate, (c) phosphate waste rock, (c) and (d) correspond to samples (a) and (b) calcined at 1,000°C.

process which made clean the samples allowing the easy access N_2 molecules to the adsorption sites. The average pore volume value (at higher relative pressure of 0.95) increased from 0.027 to 0.052 cc g^{-1}, associated with an average pore diameter of 9.58–7.62 nm, which confirms the nonporous character of the used materials. Upon calcination, a decrease of the surface area values was observed when samples were heated at 1,000°C. However, at lower temperatures of 40°C, a slight variation was reported, in good accord with the data described in the literature [44,45]. The decrease of the textural properties indicated that the thermal treatment has modified the adsorption sites to N_2 molecules compared to the original materials.

3.2. Removal studies

3.2.1. Effect of initial concentrations

The impact of varying the initial concentrations on the removed amounts by NP and PWR solids is shown in Fig. 4. The removal amount of PWR was improved from 2.03 to 85.04 mg g^{-1}, with an increase of C_i values from 10 to 250 mg L^{-1} (Fig. 5a), then it varied slightly and remained constant (90.5 mg g^{-1}) for C_i values higher than 250 mg L^{-1}. At lower concentrations, the quantity of active sites on the surface against the total dye molecules in the solution is high, therefore all of the BB-41 molecules interact with the PWR. At higher concentrations, not all the BB-41 species will be in contact with the available active surface sites [46]. Thus, a decrease of the removed amount was observed. Simultaneously, the removal percentage of BB-41 dropped from 27% to 11% with increasing the initial concentrations from 5 to 400 mg L^{-1}. Similar trends were observed for NP material with a lower uptake of 24.1 mg of BB-41/g. The removal percentages were in the range of 14% to 3% (Fig. 5b), Similar trends were reported using different solids [15,16,47].

3.2.2. Effect of calcination temperature

Fig. 5 depicts the changes of BB-41 removal efficiency when the NP and SWP were calcined at two different temperatures 400°C and 1,000°C. After calcination at 400°C, the treated waste (PWR) removed less amount of BB-41 (77.1 mg g^{-1}) compared to the pristine one (90.1 mg g^{-1}). The efficiency was significantly reduced to 54.1 mg g^{-1} when the sample was heated at 1,000°C. Similar trends were observed for the NP sample, the removal capacity for BB-41 dye was reduced from 24 to 19 to 15 mg g^{-1}. The variation in the removal properties could be related to the changes on the surfaces of the obtained materials with some loss of necessary groups to the removal of BB-41 dyes. Indeed, it was reported that the calcination process generally decreased the removal capacity for other solid waste materials [42,48].

3.2.3. Effect of solid dosage

As shown in Fig. 6, the removal efficiency of BB-41 dye was improved gradually from 22% to 99% when the mass of used PWR increased from 0.1 to 1 g, then it became unvaried even for added amounts of PWR sample higher than 1 g. However, the removal efficiency of BB-41 dye for NP material attained a value of 92%, for higher added amounts close to 1 g or above. In general, increasing the removal dosage enhances the removal efficiency of BB-41 dye and attributed to the increase of the number of available removal sites.

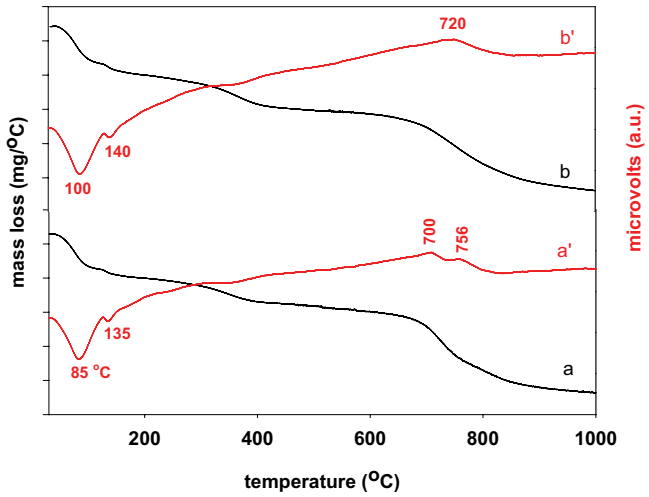

Fig. 3. Thermogravimetric analysis and differential thermal analysis of the natural phosphate (a, a′) and phosphate waste rock (b, b′) samples.

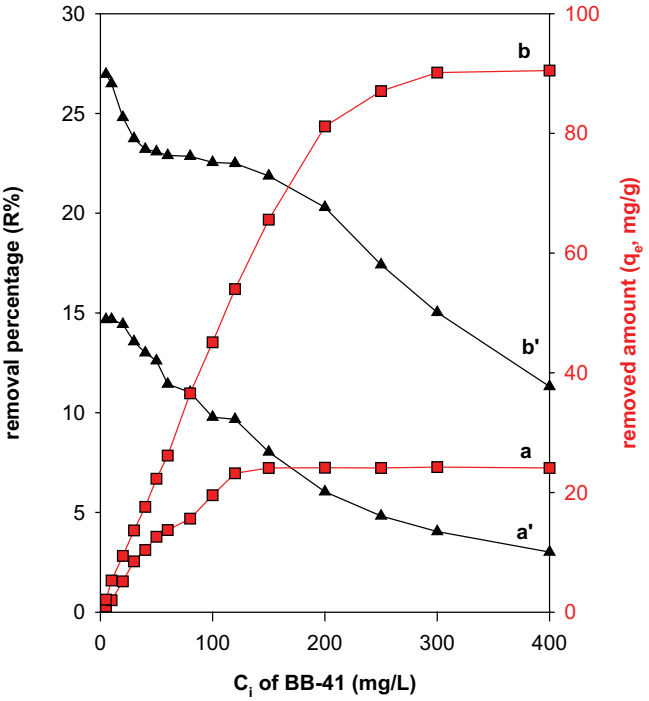

Fig. 4. Effect of Basic Blue 41 initial concentration (C_i) on the removed amounts of BB-41 (a, b) and removal percentages of (a′, b′) of NP and PWR samples, respectively. 0.1 g of the solid was added to a total volume of 200 mL (dye solution) under a shacking speed of 150 rpm, without changing the pH of the starting solution (6.50, used as natural pH) for overnight.

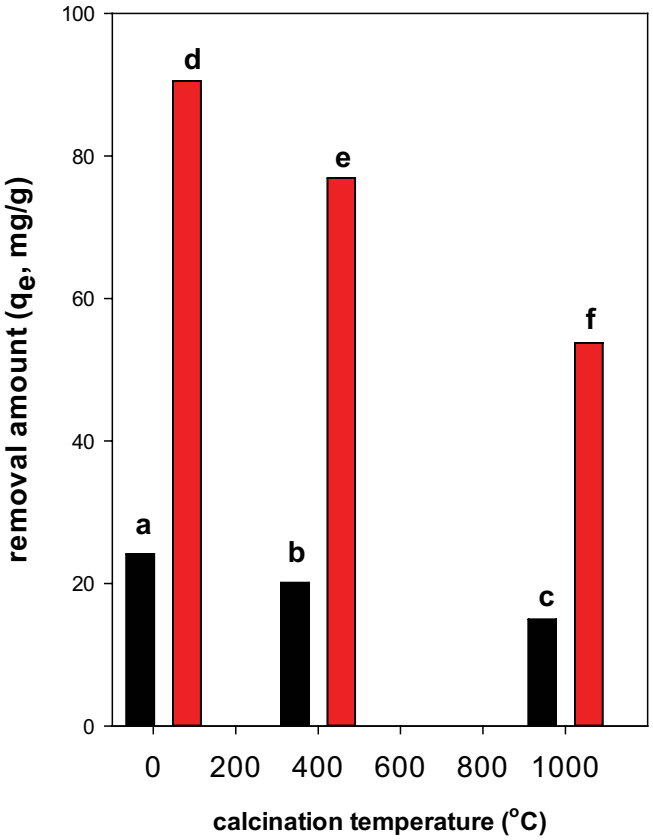

Fig. 5. Effect of calcination temperatures of NP and PWR samples on the Basic Blue 41 removal amounts, (a) for NP sample, (b) NP calcined at 400°C, and (c) calcined at 600°C, (d) natural PWR, (e) calcined at 400°C and (f) 1,000°C. Using 0.1 g of solid, volume of BB-41 solution of 200 mL, initial concentration (400 mg L^{-1}), no adjustment of pH, time (overnight), reaction temperature (25°C) and shaking rate (150 rpm).

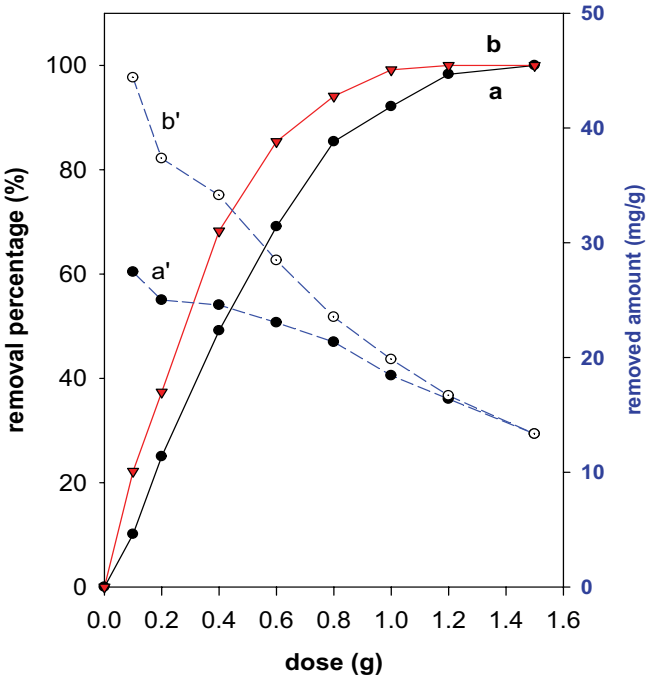

Fig. 6. Effect of NP and PWR doses on the removal amounts and percentages of BB-41 on (a, a′) NP and (b, b′) PWR samples. Using volume of BB-41 solution (200 mL), no adjustment of pH, time (overnight), reaction temperature (25°C) and shaking rate (150 rpm).

However, a decrease in the removed amount was observed from 44 to 13 mg g^{-1}, for PWR and from 27 to 13 mg g^{-1} for NP solid. This fact was extensively reported in literature. The decrease in the amount of the removed dye was the result of a considerable unsaturation of adsorption sites at high adsorbent dosages [16,30]. Even though, the PWR solid behave differently than NP sample, however, at the same dose of 1.5 g, they removed the same amount.

3.2.4. Effect of pH

The effect of pH on the adsorption of the BB-41 dye was investigated in the range from 2.5 to 11 (Fig. 7). The point of zero charge (pzc) of NP and PWR is 6.89 and 9.58, respectively. It is reported that the pH controls the molecular structure of the adsorbates and regulates the charge distribution of the adsorbents [16,49]. The removal of BB-41 was improved in the pH range of 2.5 to 7, then it remained unchanged at pH values higher than7. At pH values close to 10, the BB-41 precipitated and we were not able to carry out the experiments [16]. At acidic pH values of 2.5, lower than pH_{pzc} values, the surfaces of NP and PWR are predominantly positively charged and there is a competition between the protons release in the solution and BB-41 dye molecules which repulsing with cationic dye and competing in the adsorbent sites on NP and PWR samples. The improvement of the removal amount with the increase of initial pH values indicated a change of the positively charged surface to negatively charged surface, due to numbers of OH^- ions available on the solid surface. Thus, it enhanced the electrostatic attractions between the positively charged BB-41 dye molecules and the negatively charged surfaces, and resulted to higher dye removal efficiencies. Similar data were reported for the retention of BB-41 dye onto different solids [15,17,28,49,50].

3.2.5. Isotherms models

Several mathematical models can be used to describe experimental data of adsorption isotherms of BB-41 dye onto NP, PWR, and their derivatives calcined at 400 and 1,000°C. The equilibrium data were modeled with the Langmuir, Freundlich, Temkin, and Dubinin–Radushkevitch – D–R models) [51–54]. The linear equations of the used models are presented in Table 3. The aim of this study to find the best model that can describe the experimental results of removal BB-41, and to determine the theoretical adsorption isotherm to be used in the design purpose [55]. The calculation of all models is compiled in Table 4.

3.2.5.1. Langmuir model

This model assumes monolayer coverage of adsorbent and adsorption occurs over specific specific homogenous

sites on the adsorbent [51]. The Linear plots obtained for C_e/q_e vs. C_e (Figure not shown) with R^2 values close to 0.97 reflects that Langmuir isotherm holds quite well for BB-41 phosphate waste system. The values of the theoretical monolayer capacity q_{max} and K_L are presented in Table 3.

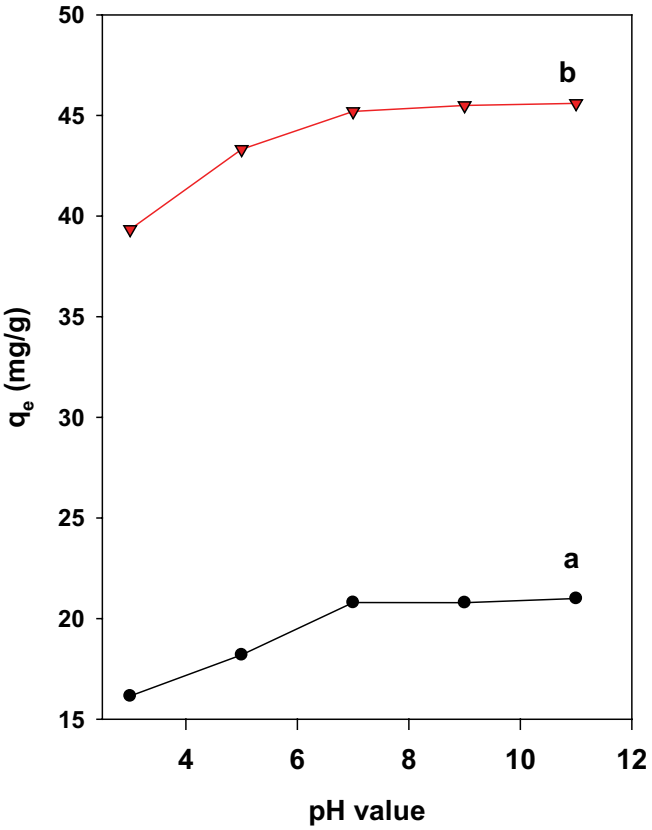

Fig. 7. pH effect of Basic Blue 41 solution on the removal properties of NP and PWR samples (a) NP and (b) PWR samples. Using 0.1 g of solid, volume of BB-41 solution of 200 mL, initial concentration (100 mg L^{-1}), time (overnight), reaction temperature (25°C) and shaking rate (150 rpm).

The values of maximum removal capacity were obtained for the WRP with value of 57.24 mg g^{-1} while the NP rock exhibited a value of 27.45 mg g^{-1}. The maximum removal capacity (q_{max}) values were not improved by the thermal treatment, and a decrease was observed.

3.2.5.2. Freundlich model

The Freundlich model endorses the existence of active sites on the adsorbent with a very heterogeneous energetic distribution [52].

K_F is a combined measure of both the adsorption capacity and affinity, and $1/n$ indicates the degree or intensity of the removed BB-41 dye. The favorability of the removal is indicated by the magnitude of n, that is, values of [55]. Table 4 indicates that the experimental data fitted better within this model with values of R^2 close to 1 and were the highest compared to the other models, and indicated that the surface of the used waste materials is not very homogenous in comparison to the Langmuir model, and a multilayer adsorption on the surface is envisaged.

The highest value of K_F was obtained for the PWR solid, accompanied with a decrease when the sample was heat treated, indicating a decrease in dye – adsorbent interaction when the wastes were treated at higher temperatures prior the removal process. The values of n were found to be greater than 1 for all the used samples without or with pre-thermal treatment, which may be attributed to the distribution of surface sites or any factor responsible for a decrease in dye-solid interaction with increasing surface density.

3.2.5.3. Temkin model

The Temkin isotherm model contains a factor that explicitly takes into account the interactions between adsorbate and adsorbent species [53,55].

In our case, the values of R^2 were the lower, and varied between 0.93 and 0.96. The highest values (0.96) were obtained for NP solid sample (Table 4), and suggested that this model did not satisfy the experimental data.

Table 3
Equations of the used models [51–54]

Isotherm models	Linear expression	Parameters
Langmuir [51]	$\frac{1}{q_e}=\frac{1}{q_m}+\frac{1}{K_L q_m}C_e$	q_e (mg g^{-1}), C_e (mg L^{-1}), K_L is Langmuir constant (L mg^{-1}), and q_m maximum adsorption capacity (mg g^{-1}).
Freundlich [52]	$q_e=\log K_F+\frac{1}{n}\log C_e$	q_e (mg g^{-1}), C_e (mg L^{-1}), K_F (L mg^{-1}) Freundlich constant and n is the dimensionless factor.
Temkin model [53]	$q_e=B\ln A_T+B\ln C_e$	q_e (mg g^{-1}), C_e (mg L^{-1}), A_T, Temkin equilibrium constant (L g^{-1}), B = related to heat of sorption (kJ mol^{-1})
Dubinin–Radushkevitch model [54]	$\ln q_e=\ln q_m-\beta\varepsilon^2$ $\varepsilon=RT\ln\left[1+\left(\frac{1}{C_e}\right)\right]$	q_e (mg g^{-1}), q_m is the D–R monolayer capacity (mg g^{-1}), β is the activity coefficient related to mean sorption energy (mol² kJ^{-2}) and ε is the Polanyi potential. R is the gas constant (8.314 J mol^{-1} K^{-1}) and T is the temperature in K.

Table 4
Calculated adsorption isotherm values using regression analysis for BB-41 removal

Mathematical model	Parameters	NP	NP-400	NP-1000	WPS	WPS-400	WPS-1000
Langmuir	R^2	0.974	0.962	0.811	0.920	0.925	0.899
	q_{max} (mg g^{-1})	57.2	33.6	23.6	207.2	162.3	116.1
	K_L (L mg^{-1})	2.50×10^{-3}	2.91×10^{-3}	2.77×10^{-3}	4.71×10^{-3}	8.09×10^{-3}	9.34×10^{-3}
Freundlich	R^2	0.978	0.976	0.903	0.990	0.989	0.990
	K_F (mg g^{-1})(L mg)$^{-1/n}$	0.300	0.230	0.180	0.652	0.534	0.388
	$1/n$	0.890	0.895	0.890	0.903	0.904	0.903
Temkin	R^2	0.969	0.968	0.963	0.937	0.934	0.937
	B_T (kJ mol^{-1})	347.38	431.81	576.05	102.82	120.55	172.81
	A_T (L mg^{-1})	0.136	0.136	0.136	0.087	0.086	0.087
Dubinin–Radushkevitch	R^2	0.851	0.855	0.850	0.761	0.752	0.760
	q_m (mg g^{-1})	13.80	11.03	8.27	38.36	32.08	22.83
	K	1.468×10^{-5}	1.467×10^{-5}	1.46×10^{-5}	1.613×10^{-5}	1.612×10^{-5}	1.61×10^{-5}
	E (J mol^{-1})	185.05	184.59	184.54	176.17	176.19	176.22

Nevertheless, the Temkin constant, B_T related to heat of sorption for the BB-41 dye varied between 102 and 576 J mol^{-1}, and indicated physical adsorption as they are less than 8 kJ mol^{-1} for all dye-waste phosphate systems [55]

Moreover, the heat of adsorption of natural PWR was greater than the heat of adsorption of thermal treated of PWR, this implied that interactions between BB-41 and natural PWR were more energetic than interactions between BB-41 and thermal treated wastes.

3.2.5.4. Dubinin–Radushkevitch model

The D–R isotherm model is applied to estimate the apparent free energy and characteristics of adsorption. The linear form of D–R isotherm [54,55].

The mean adsorption energy, E (kJ mol^{-1}) was calculated with the help of the following equation:

$$E = \frac{1}{\sqrt{(-2\beta)}} \tag{4}$$

As presented in Table 4, the R^2 values were not too high and they were the lowest compared to the three described models above, they varied from 0.76 to 0.85, and indicated that this model was not adequate to describe the removal of BB-41 dyes by the solid wastes. Nevertheless, the values of E (the mean free energy of adsorption) were in the range of 172 to 185 J mol^{-1}, and suggested that physiosorption played a significant role in the removal process of BB-41 dye, when the phosphate materials were used.

In overall, the highest values of R^2 were obtained for the Freundlich model, and indicated that the removal data best fitted the Frendlich adsorption isotherm. The good fit of Freundlich suggested that this isotherm is appropriate under industrial conditions.

3.2.6. Effect of removal temperature

The effect of temperature on the adsorbed amount of NP and PWR were investigated. The results revealed that the amount of BB-41 adsorbed increased with increasing temperature. The thermodynamic parameters of the adsorption reaction were computed from the achieved experimental results using the following equations [56,57]:

$$\Delta G = \Delta H - T\Delta S \tag{5}$$

$$\Delta G_{ads} = -RT \ln K_c \tag{6}$$

$$\ln K_c = \left(\frac{\Delta S}{R}\right) - \left(\frac{\Delta H}{R}\right)\frac{1}{T} \tag{7}$$

where K_c is the distribution coefficient of BB-41, T is the temperature in Kelvin, and R is the gas constant. ΔG is the free energy change, ΔS is the entropy change of adsorption, and ΔH is enthalpy change. The values of ΔH and ΔS were determined from the slope of the linear plot of $\ln K_d$ vs. $1/T$ and the free energy change ΔG was calculated from Eq. (5) at 303 K and given in Table 5.

The positive value of the enthalpy (ΔH) indicated that the phenomenon is endothermic which is consistent with the increasing removal capacity with temperature values [56]. Also, the positive value of ΔS accompanying the removal of BB-41 reveals the increased randomness at the solid–solution interface during the fixation of the ion on the surface of the sorbent. The negative values of ΔG indicated the spontaneous nature of the removal process. Similar data were reported for different used adsorbents.

3.2.7. Comparison of the q_{max} by different adsorbents

The maximum removal capacity (q_{max}) obtained in this study were compared to those reported in the literature for a variety of adsorbents (Table 6). The waste phosphate (PWR) exhibited good removal efficiency, and it could be used as a potential candidate.

4. Theoretical calculation and possible interaction

It was well established that the adsorption is a surface effect, and it can be categorized into physical or chemical

adsorption, according to the different types of interaction between adsorbent and adsorbate [62].

For the physical adsorption, the main interactions are the VDW (Van der Waals' forces) between the adsorbent and adsorbate. Because there is no chemical bonds produce between the waste products and BB-41 dyes. The possible forms of the physical adsorption process would be hydrogen bonds, electrostatic effect. The main factors that affected the physical adsorption process are those: the electric intensity of hydrogen bond donor and acceptor; the steric hindrance intensity of adsorbate; the electrostatic effect etc. [63].

In this study, the possible interaction sites through computation of electronic charge distribution and electrostatic potential was investigated. The interactions between phosphate groups (PO_4^{-3}) of PWR solid and BB-41 dye is considered as background knowledge due to (a) acid–base interaction due to hydrogen bonding; (b) adsorption by dispersion forces as a principle of electrostatic interactions; and (c) ion pairing by adsorption onto oppositely unoccupied charged sites [27]

Mulliken atomic charges calculated by the semi-empirical PM3 theoretical method shows that, for BB-41dye, the most of the negative charges were centered onto the oxygen atoms and some nitrogen atoms, while, the positive charges were situated on other nitrogen and sulfur atoms. In other words, the half side of the molecule with sulfur and nitrogen heteroatom's is more positively charged. It should also be noted that the positive charge on the hydrogen atom of the hydroxyl group (OH) in the second half of the molecule has a very marked positive charge (0.2 e^-) [64]. The electrostatic potential (ESP) is important for understanding the chemical reactivity and the atomic structure of molecules and solids [65]. It is useful for finding sites of interaction in a molecule: negatively charged species which tend to attack the sites where the electrostatic potential is strongly positive. The three-dimension (3D) mapped isosurface of the electrostatic potential surrounding BB-41 molecule. Indicated the presence of weak positive ESP regions, followed by slightly positive ESP, and blue strong positive ESP regions [64].

In the case of electrostatic attraction with a negatively charged surface like phosphate (PO_4^{-2}), the BB-41 molecules would have a tendency to orient themselves preferentially to the surface by the sides possessing the highest values of positive charge density. The orientation via the hydrogen of alkyl amine group $–NCH_3$ situated in the first half of the molecule or to the orientation with cycle having the suffer (S) atom. Finally, orientation with the hydrogen of hydroxyl group of the second side of the molecule was not excluded. In all cases the orientation positions of BB-41 are parallel and anti-parallel with respect to the negatively charged surface of the phosphate, as presented in Fig. 8a and b.

Table 5
Thermodynamic parameters for the removal of Basic Blue 41 onto various samples

Samples	ΔH (kJ mol^{-1})	ΔS (J mol^{-1} K^{-1})		R^2
NP	8.166	41.535		0.999
PWR	17.131	58.897		0.994
T (K)	308	318	333	348
		ΔG (kJ mol^{-1})		
NP	–4.419	–5.042	5.665	–6.288
PWR	–0.715	–1.598	2.482	–3.365

5. Regeneration data

The recycle of adsorbent is a very important and crucial factor to propose an efficient adsorbent. Good adsorbent is supposed to have high removal capacity and regeneration efficiency [66].

Different methods of regeneration were reported in the literature, including two ways, washing of the used samples with different ethanol, acidic or basic solutions to remove the adsorbed dyes as they are [66,67], or to destroy the adsorbed dyes by thermal treatment at certain temperatures [67], this process will add additional costs to the process due the extra energy consumption. Another method was proposed by other researchers to destroy the adsorbed dyes on the surface of the solids via sulphate radical oxidation. This method was reported to be friendly to the environment since the solution could be used for many regeneration tests [15].

As presented in Fig. 9, the removal efficiency is reduced to some extent from 68% to 58%, for the PWR sample after four runs. However, for the other sample NP, its removal percentage decreased from 24% to 15% after third regeneration cycle. Overall, the removal efficiency is maintained up to 61% of the original value for the sixth regeneration cycle. This drop in efficiency could indicate that some BB-41 molecules were strongly attached to the surface of the solid, thus made their decomposition difficult during the regeneration process [16]. However, for the calcined wastes the data indicated that a reasonable removal efficiency was maintained only for 2 cycles, then a drastic decrease was observed to 40%–50% of the original value. This decrease was due to the starting low removal percentage values for the calcined materials

6. Batch design from Freundlich isotherm data

The Adsorption isotherms were used to predict the proposal of single-stage batch adsorption systems [68–70].

Table 6
Maximum removal capacity (q_{max}) of BB-41 by different materials

Adsorbent	q_{max} (mg g^{-1})	Reference
Waste phosphate rock	207	This study
Natural phosphate rock	57	This study
Raw waste bricks Medina	30	[58]
Raw waste bricks Jeddah	19	[15]
Modified waste bricks Medina	60	[58]
Modified waste bricks Jeddah	32	[15]
Local clay	73	[16]
Acid activated local clay	50	[16]
Jordanian kaolinite	6	[59]
Natural zeolitic tuff	39	[60]
Mn modified diatomite	62	[61]

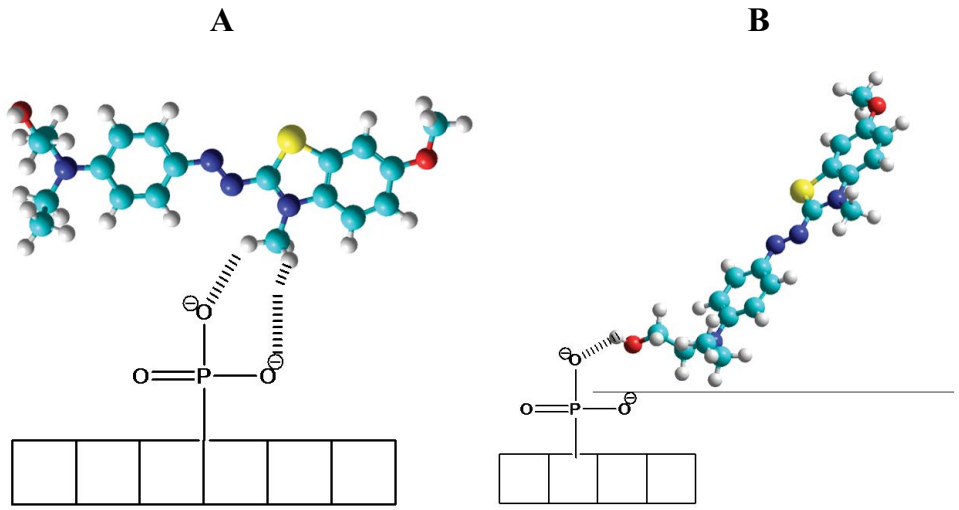

Fig. 8. Possible schematic presentation of the removal process of Basic Blue 41 onto phosphate waste material. (A) Parallel orientation and (B) anti-parallel orientation of BB-41 molecule.

The design objective was to predict the required amount of adsorbents (M (g)) necessary to reduce the concentration of BB-41 dye from C_0 (mg L^{-1}) to C_1 (mg L^{-1}) at specific wastewater volume (L) [28]. The removed BB-41 (mg dye per g of solid) varies from q_0 (mg g^{-1}) to q_1 (mg g^{-1}). The mass balance at equilibrium condition is given as:

$$V\left(C_0 - C_e\right) = m\left(q_0 - q_e\right) = mq_e \tag{8}$$

In the present case the removal of BB-41 fitted well with Freundlich isotherm. As a result, can be substituted in Eq. (5), and the rearranged form is presented in Eq. (6) [65].

$$\frac{m}{V} = \frac{C_0 - C_e}{q_e} = \frac{C_0 - C_e}{K_F C_e^{1/n}} \tag{9}$$

Replacing $C_0 - C_e$ and C_e expressions by C_0, Eq. (9) could be rewritten as

$$\frac{m}{V} = \frac{C_0 - C_e}{q_e} = \frac{RC_0}{K_F\left((1-R)C_0\right)^{1/n}} \tag{10}$$

Fig. 10A illustrates the plots derived from Eq. (10) to predict the required amount of PWR (g) to reduce the C_i of 200 mg L^{-1} to 50%, 60%, 70%, 80%, and 90%, from different volumes of BB-41 in the range of 1–12 L in 1 L increment. In general, the required mass of PWR and NP increased with the raise of used volumes of the effluent and desired removal percentage values (Fig. 10A and 10A′). The reduction of a fixed volume of 10 L with a C_i of 200 mg L^{-1}) to 100, 120, 140, 160, and 180 mg L^{-1}, required 71.9, 105.2, 158.5, 260.1 and 542.0 g, respectively, when NP is used. However, for the same process, the predicted amounts of PWR were 30.7, 45.2, 68.3, 112.6, and 236.9 g, respectively for PWR sample.

As we have mentioned above, the predicted masses of PWR solid were always lower than those of NP materials, due to the difference in their removal properties (Fig. 10A′).

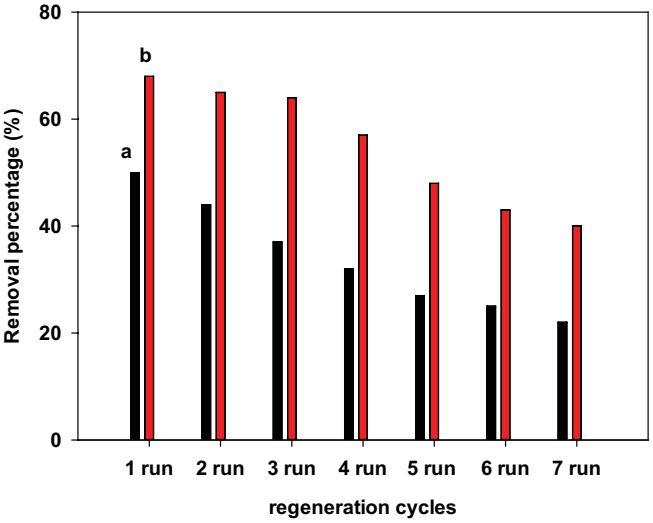

Fig. 9. Regeneration studies of (a) NP and (b) PWR samples.

Similar behavior was observed for the calcined NP and PWR materials at 400°C and 1,000°C. These findings can be explored to remove BB-41 dye on large scale level.

7. Conclusions

The by-product regenerated from the phosphate mining after washing process was used as removal agent of BB-41 dye, it exhibited higher removal capacity (207.2 mg g^{-1}) than the raw natural phosphate rock (57.2 mg g^{-1}). The pre-thermal treatment of PWR resulted in the reduction of the waste efficacy of about 50%. The removed amount of BB-41 dye depended on many factors and especially on pH values of the starting solution. The experimental data fitted well Freundlich model isotherm suggesting heterogeneity of the surface. The removal of BB-41 molecules was spontaneous and endothermic process. About 80% of the

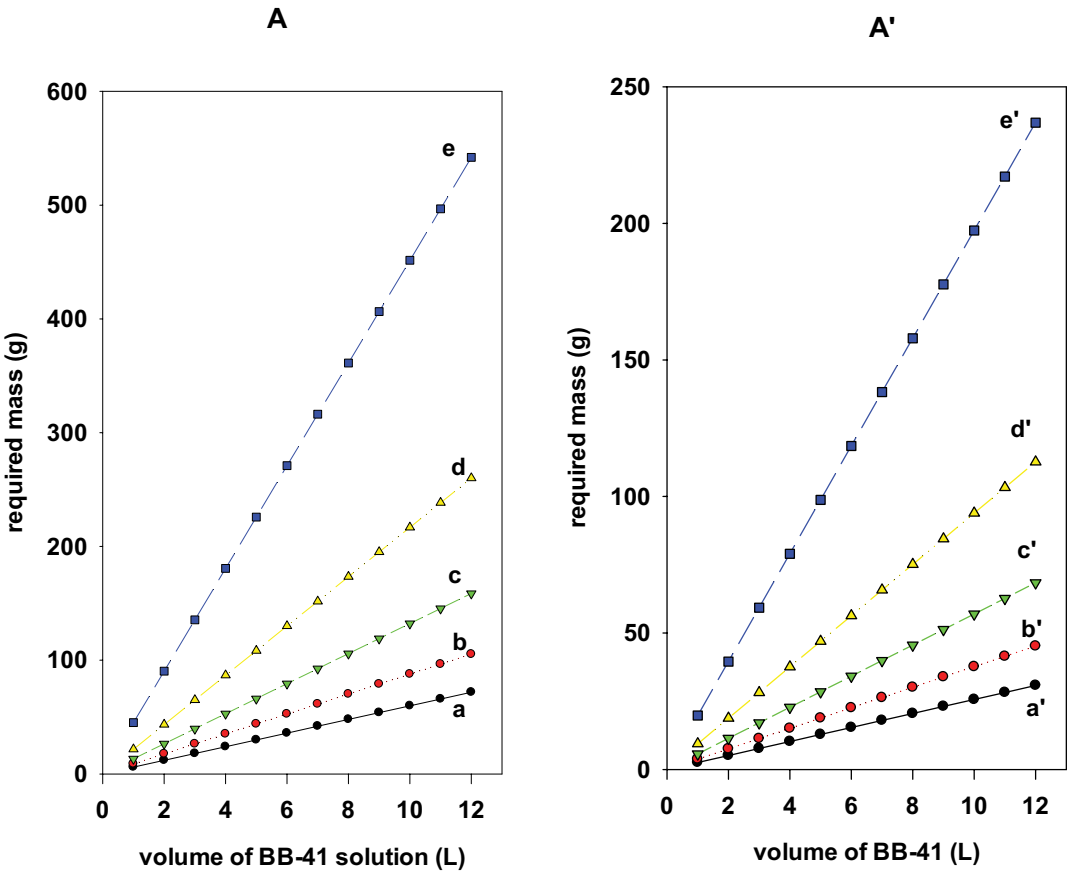

Fig. 10. Design plot generated using Freundlich isotherm for (A) NP and (A′) PWR samples to treat different effluent (L) of BB-41 at removal percentages. (a, a′) 50%, (b, b′) 60%, (c, c′) 70%, (d, d′) 80%, and (e, e′) 80%, for a fixed C_i of 200 mg L^{-1}.

removed amount was retained after four cycles, and it was reduced to 60% after its reuse for seven repeating cycles, for all the spent materials and for C_i value of 200 mg L^{-1}. Based on the Freundlich equilibrium data, batch adsorber design was proposed to determine the minimum amount of the adsorbent required to remove a given amount of dye from a fixed initial dye solution in a defined volume. These data suggested that the waste by-products of phosphate mining are a potential candidate for the treatment of colored polluted water. Dye containing wastewater is not a single component system hence, the effect of other contaminants like surfactant, salinity on dye removal process by the adsorbent plays an important role, and it should be taken in account to complete this investigation.

Acknowledgement

The authors would like to thank Dr. Nouar Sofiane Labidi from the University Centre of Tamanrasset, Algeria, for his help and calculation of the Mulliken atomic charges and electrostatic potential of Basic Blue 41 dye.

References

[1] K. Hunger, Industrial Dyes: Chemistry, Properties, Applications, Wiley-Verlag GmbH & Co., Weinheim, 2003.
[2] O.M.L. Alharbi, A.A. Basheer, R.A. Khattab, I. Ali, Health and environmental effects of persistent organic pollutants, J. Mol. Liq., 263 (2018) 442–453.
[3] S.J. Culp, F.A. Beland, Malachite green: a toxicological review, Int. J. Toxicol., 15 (1996) 219–238.
[4] A.E. Ghaly, R. Ananthashankar, M. Alhattab, V.V. Ramakrishnan, Production, characterization and treatment of textile effluents: a critical review, J. Chem. Eng. Process. Technol., 5 (2014) 182–200.
[5] A. Rossner, S.A. Snyder, D.R.U. Knappe, Removal of emerging contaminants of concern by alternative adsorbents, Water Res., 43 (2009) 3787–3796.
[6] S. Venkata Mohan, P. Sailaja, M. Srimurali, J. Karthikeyan, Colour removal of monoazo acid dye from aqueous solution by adsorption and chemical coagulation, Environ. Eng. Policy, 1 (1999) 149–154.
[7] G. Crini, Non-conventional low-cost adsorbents for dye removal: a review, Bioresour. Technol., 97 (2006) 1061–1085.
[8] M. Muthukumar, D. Sargunamani, N. Selvakumar, Statistical analysis of the effect of aromatic, azo and sulphonic acid groups on decolouration of acid dye effluents using advanced oxidation processes, Dyes Pigm., 65 (2005) 151–158.
[9] M.S. Khehra, H.S. Saini, D.K. Sharma, B.S. Chadha, S.S. Chimni, Biodegradation of azo dye C.I. Acid Red 88 by an anoxic–aerobic sequential bioreactor, Dyes Pigm., 70 (2006) 1–7.
[10] C. O'Neill, A. Lopez, S. Esteves, F.R. Hawkes, D.L. Hawkes, S. Wilcox., Azo-dye degradation in an anaerobic-aerobic treatment system operating on simulated textile effluent, Appl. Microbiol. Biotechnol., 53 (2000) 249–254.
[11] M.T. Yagub, T.K. Sen, S. Afroze, H.M. Ang, Dye and its removal from aqueous solution by adsorption: a review, Adv. Colloid Interface Sci., 209 (2014) 172–184.

[12] R. Ozdogan, M. Celebi, Elimination of Basic Blue 41 ve Basic Red 46 dyestuffs from solution by anionic polymer membrane, Acad. Platform-J. Eng. Sci., 6 (2018) 17–24.
[13] M. Wakkel, B. Khiari, F. Zagrouba, Textile wastewater treatment by agro-industrial waste: equilibrium modelling, thermodynamics and mass transfer mechanisms of cationic dyes adsorption onto low-cost lignocellulosic adsorbent, J. Taiwan Inst. Chem. Eng., 96 (201) 439–452.
[14] H. Faraji, A.A. Mohamadi, S. Arezomand, H. Reza, A.H. Mahvi, Kinetics and equilibrium studies of the removal of blue basic 41 and methylene blue from aqueous solution using rice stems, Iran. J. Chem. Chem. Eng., 34 (2015) 33–42.
[15] F. Kooli, Y. Liu, M. Abboudi, H. Hassani Oudguiri, S. Rakass, S.M. Ibrahim, F. Al Wadaani, Waste bricks applied as removal agent of Basic Blue 41 from aqueous solutions: base treatment and their regeneration efficiency, Appl. Sci., 9 (2019) 1237, doi: 10.3390/app9061237.
[16] F. Kooli, L. Yan, R. Al-Faze, A. Al Suhaimi, Effect of acid activation of Saudi local clay mineral on removal properties of Basic Blue 41 from an aqueous solution, Appl. Clay Sci., 116–117 (2015) 23–30.
[17] C. Aguir, M.F. M'henni, Removal of Basic Blue 41 from aqueous solution by carboxymethylated *Posidonia oceanica*, J. Appl. Polym. Sci., 103 (2007) 1215–1225.
[18] A. Nakhli, M. Bergaoui, C. Aguir, M. Khalfaoui, M.F. M'henni, A. Ben Lamine, Adsorption thermodynamics in the framework of the statistical physics formalism: Basic Blue 41 adsorption onto *Posidonia* biomass, Desal. Water Treat., 57 (2016) 12730–12742.
[19] A. Regti, M.R. Laamari, S.E. Stiriba, M.E. El Haddad, Removal of Basic Blue 41 dyes using *Persea americana*-activated carbon prepared by phosphoric acid action, Int. J. Ind. Chem., 8 (2017) 187–195.
[20] N. Abbes, E. Bilal, L. Hermann, G. Steiner, N. Haneklaus, Thermal beneficiation of Sra Ouertane (Tunisia) low-grade phosphate rock, Minerals, 10 (2020) 937–950.
[21] D. McConnell, A structural investigation of the isomorphism of the Apetite Group, Am. Mineral., 23 (1938) 1–19.
[22] P. Zhang, J.D. Miller, H.E. El-Shall, Beneficiation of Phosphates: New Thought, New Technology, New Development, Publisher Englewood, Colo. Society for Mining, Metallurgy, and Exploration, 2012.
[23] N.S. Awwad, Y.A. El-Nadi, M.M. Hamed, Successive processes for purification and extraction of phosphoric acid produced by wet process, Chem. Eng. Process. Process Intensif., 74 (2013) 69–74.
[24] H. Tayibi, M. Choura, F.A. López, F.J. Alguacil, A. López-Delgado, Environmental impact and management of phosphogypsum, J. Environ. Manage., 90 (2009) 2377–2386.
[25] Z. Graba, S. Hamoudi, D. Bekka, N. Bezzi, R. Boukherroub, Influence of adsorption parameters of basic red dye 46 by the rough and treated Algerian natural phosphates, J. Ind. Eng. Chem., 25 (2014) 229–238.
[26] A. Aklil, M. Mouflih, S. Sebti, Removal of heavy metal ions from water by using calcined phosphate as a new adsorbent, J. Hazard. Mater., 112 (2004) 183–19.
[27] N.S. Labidi, N.E. Kacemi, Adsorption mechanism of malachite green onto activated phosphate rock: a kinetics and theoretical study, Bull. Environ. Stud., 1 (2016) 69–74.
[28] K. Boughzala, F. Kooli, N. Meksi, A. Bechrifa, K. Bouzouita. Waste products from the phosphate industry as efficient removal of Acid Red 88 dye from aqueous solution their regeneration uses and batch design adsorber, Desal. Water Treat., 202 (2020) 410–419.
[29] M.A. Rauf, I. Shehadeh, A. Ahmed, A. Al-Zamly, Removal of Methylene Blue from aqueous solution by using gypsum as a low cost adsorbent, World Acad. Sci. Eng. Technol., 3 (2009) 540–545.
[30] Y. Wu, J. Cao, P. Yilihan, Y. Jin, Y. Wen, J. Zhou, Adsorption of anionic and cationic dyes from single and binary systems by industrial waste lead–zinc mine tailings, RSC Adv., 3 (2013) 10745–10753.
[31] N. Barka, A. Assabbane, A. Nounah, L. Laanab, Y. Aît Ichou, Removal of textile dyes from aqueous solutions by natural phosphate as a new adsorbent, Desalination, 235 (2009) 264–275.
[32] Z. Elouear, J. Bouzid, N. Boujelben, M. Feki, F. Jamoussi, A. Montiel, Heavy metal removal from aqueous solutions by activated phosphate rock, J. Hazard. Mater., 156 (2008) 412–420.
[33] E. Keleş, A.K. Özer, S. Yörük, Removal of Pb^{2+} from aqueous solutions by phosphate rock (low-grade), Desalination, 253 (2010) 124–128.
[34] N.S. Labidi, N.E. Kacemi, Equilibrium modelling and kinetic studies on the adsorption of basic dye by natural and activated algerian phosphate rock, Environ. Res. Int., 2 (2016) 1–6.
[35] A.Z.M. Abouzied, Physical and thermal treatment of phosphate ores – an overview, Int. J. Miner. Process., 85 (2008) 59–84.
[36] H.H. Lim, Beneficiation of apatite rock phosphates by calcination: effects on chemical properties and fertilizer effectiveness, Aust. J. Soil Res., 39 (2001) 397–402.
[37] W. Baran, A. Makowski, W. Wardas, The influence of $FeCl_3$ on the photocatalytic degradation of dissolved azo dyes in aqueous TiO_2 suspensions, Chemosphere, 53 (2003) 87–95.
[38] I. Bouatba, L. Bilali, M. Benchanaa, M. El-Hammioui, Decadmiation of natural phosphates by heat treatment and hydrochloric acid, Asian J. Chem., 28 (2016) 819–824.
[39] A. Mizane, A. Louhi, Calcination effects on sulfuric dissolution of phosphate extracted from Djebel Onk Mine (Algeria), Asian J. Chem., 20 (2008) 711–717.
[40] N. Gmati, K. Boughzala, M. Abdellaoui, K. Bouzouita, Mechanochemical synthesis of strontium britholites: reaction mechanism, C.R. Chim., 14 (2011) 896–903.
[41] J.P. Lafon, E. Champion, D. Bernache-Assollant, Processing of AB-type carbonated hydroxyapatite $Ca_{10-x}(PO_4)_{6-x}(CO_3)_x(OH)_{2-x-2y}(CO_3)_y$ ceramics with controlled composition, J. Eur. Ceram. Soc., 28 (2008) 139–147.
[42] Z. Graba, S. Hamoudi, D. Bekka, N. Bezzi, R. Boukherroub, Influence of adsorption parameters of basic red dye 46 by the rough and treated Algerian natural phosphates, J. Ind. Eng. Chem., 25 (2015) 229–238.
[43] H. Bouyarmane, S. Saoiabi, A. Laghzizil, A. Saoiabi, A. Rami, M. El-Karbane, Natural phosphate and its derivative porous hydroxyapatite for the removal of toxic organic chemicals, Desal. Water Treat., 52 (2014) 7265–7269.
[44] A. Mgaidi, F. Ben Brahim, D. Oulahna, A. Nzihou, M. El Maaoui, Chemical and structural changes of raw phosphate during heat treatment, High Temp. Mater. Processes, 23 (2004) 185–194.
[45] T.F. Al-Fariss, F.A. Abd El-Aleem, Y. Arafat, K.A. El-Nagdy, A.A. El-Midany, Low solubility of calcined phosphate: surface area reduction or chemical composition change?, Part. Sci. Technol., 32 (2014) 80–85.
[46] A. Achkoun, J. Naja, R. M'Hamdi, Elimination of cationic and anionic dyes by natural phosphate, J. Chem. Chem. Eng., 6 (2012) 721–725.
[47] G.L. da Silva, V.L. Silva, M.G.A. Vieira, M.G.C. da Silva, Solophenyl navy blue dye removal by smectite clay in a porous bed column, Adsorpt. Sci. Technol., 27 (2009) 861–876.
[48] V. Vimonses, B. Jin, C.W.K. Chow, C. Saint, Enhancing removal efficiency of anionic dye by combination and calcination of clay materials and calcium hydroxide, J. Hazard. Mater., 171 (2009) 941–947.
[49] H. El Boujaady, A. El Rhilassi, M. Bennani-Ziatni, R. El Hamri, A. Taitai, J.L. Lacout, Removal of a textile dye by adsorption on synthetic calcium phosphates, Desalination, 275 (2011) 10–16.
[50] S. Rakass, H. Oudghiri Hassani, M. Abboudi, F. Kooli, A. Mohmoud, A. Aljuhani, F. Al Wadaani, Molybdenum trioxide: efficient nanosorbent for removal of methylene blue dye from aqueous solutions, Molecules, 23 (2018) 2295–2308.
[51] I. Langmuir, The adsorption of gases on plane surfaces of glass, mica and platinum, J. Am. Chem. Soc., 40 (1918) 1361–1403.
[52] H.M.F. Freundlich, Over the adsorption in solution, J. Phys. Chem., 57 (1906) 385–470.
[53] M.I. Temkin, Adsorption equilibrium and the kinetics of processes on non-homogeneous surfaces and in the interaction between adsorbed molecules, Zh. Fiz. Chim., 15 (1941) 296–332.

[54] M.M. Dubinin, E.D. Zaverina, L.V. Radushkevich, Soprtion and structure of activated carbons. I. Adsorption of organic vapours, J. Phys. Chem., 21 (1947) 1351–1362.
[55] M.A. Al-Ghouti, D.A. Daana, Guidelines for the use and interpretation of adsorption isotherm models: a review, J. Hazard. Mater., 393 (2020) 122383–122405.
[56] C.-H. Wu, Adsorption of reactive dye onto carbon nanotubes: equilibrium, kinetics and thermodynamics, J. Hazard. Mater., 144 (2007) 93–100.
[57] A. Ramesh, D.J. Lee, J.W. Wong, Thermodynamic parameters for adsorption equilibrium of heavy metals and dyes from wastewater with low cost adsorbents, J. Colloid Interface Sci., 291 (2005) 588–592.
[58] F. Kooli, L. Yan, R. Al-Faze, A. Al-Sehimi, Removal enhancement of Basic Blue 41 by waste brick from an aqueous solution, Arabian J. Chem., 8 (2015) 333–342.
[59] M. Gougazeh, F. Kooli, J.-Ch. Buhl, Removal efficiency of basicblue41 by three zeolites prepared from natural Jordanian kaolinite, Clays Clay Miner., 67 (2019) 143–153.
[60] I. Humelnicu, A. Baiceanu, M.E. Ignat, V. Dulman, The removal of Basic Blue 41 textile dye from aqueous solution by adsorption onto natural zeolitic tuff: kinetics and thermodynamics, Process Saf. Environ. Prot., 105 (2017) 274–287.
[61] A.R. Kul, A. Aldemir, H. Koyuncu, An investigation of natural and modified diatomite performance for adsorption of Basic Blue 41: isotherm, kinetic, and thermodynamic studies, Desal. Water Treat., 229 (2021) 384–394.
[62] N. Saad, M. Al-Mawla, E. Moubarak, M. Al-Ghoul, H. El-Rassy, Surface-functionalized silica aerogels and alcogels for methylene blue adsorption, RSC Adv., 5 (2015) 6111–6122.
[63] H. Han, W. Wei, Z. Jiang, J. Lu, J. Zhu, J. Xie, Removal of cationic dyes from aqueous solution by adsorption onto hydrophobic/hydrophilic silica aerogel, Colloids Surf., A, 509 (2016) 539–549.
[64] H. Al Dmour, F. Kooli, A. Mohmoud, L. Yan, S.A. Popoola, Al and Zr porous clay heterostructures as removal agents of Basic Blue 41 dye from an artificially polluted solution: regeneration properties and batch design, Materials, 14 (2021) 2528, doi: 10.3390/ma14102528.
[65] P. Politzer, J.S. Murray, M.C. Concha, The complementary roles of molecular surface electrostatic potentials and average local ionization energies with respect to electrophilic processes, Quantum Chem., 88 (2002) 19–27.
[66] T.P.K. Kulasooriya, N. Priyantha, A.N. Navaratne, Removal of textile dyes from industrial effluents using burnt brick pieces: adsorption isotherms, kinetics and desorption, SN Appl. Sci., 2 (2020) 1789, doi: 10.1007/s42452-020-03533-0.
[67] S. Wang, H. Li, S. Xie, S. Liu, L. Xu, Physical and chemical regeneration of zeolitic adsorbents for dye removal in wastewater treatment, Chemosphere, 65 (2006) 82–87.
[68] S. Dawood, T.K. Sen, Removal of anionic dye Congo red from aqueous solution by raw pine and acid-treated pine cone powder as adsorbent: equilibrium, thermodynamic, kinetics, mechanism and process design, Water Res., 46 (2012) 1933–1946.
[69] Y. Khambhaty, K. Mody, S. Basha, Efficient removal of Brilliant Blue G (BBG) from aqueous solutions by marine *Aspergillus wentii*: kinetics, equilibrium and process design, Ecol. Eng., 41 (2012) 74–83.
[70] V.O. Shikuku, R. Zanella, C.O. Kowenje, F.F. Donato, N.M.G. Bandeira, O.D. Prestes, Single and binary adsorption of sulfonamide antibiotics onto iron-modified clay: linear and nonlinear isotherms, kinetics, thermodynamics, and mechanistic studies, Appl. Water Sci., 8 (2018) 175–187.